

## Systematic study of short-range antiferromagnetic order and the spin-glass state in lightly doped $\text{La}_{2-x}\text{Sr}_x\text{CuO}_4$

S. Wakimoto,\* S. Ueki, and Y. Endoh

*Department of Physics, Tohoku University, Sendai 980-8578, Japan*

K. Yamada

*Institute for Chemical Research, Kyoto University, Gokasho, Uji 610-0011, Japan*

(Received 25 October 1999)

Systematic measurements of the magnetic susceptibility were performed on single crystals of lightly doped  $\text{La}_{2-x}\text{Sr}_x\text{CuO}_4$  ( $x=0.03, 0.04, \text{ and } 0.05$ ). For all samples the temperature dependence of the in-plane magnetic susceptibility shows typical spin-glass features with spin-glass transition temperatures  $T_g$  of 6.3, 5.5, and 5.0 K for  $x=0.03, 0.04, \text{ and } 0.05$ , respectively. The canonical spin-glass order parameter extracted from the in-plane susceptibility of all the samples follows a universal scaling curve. On the other hand, the out-of-plane magnetic susceptibility deviates from Curie law below a temperature  $T_{dv}$ , higher than  $T_g$ . Comparing with previous neutron-scattering results with an instrumental energy resolution of  $\Delta\omega\sim 0.25$  meV from Wakimoto *et al.*, the  $x$  dependence of  $T_{dv}$  is qualitatively the same as that of  $T_{el}$  ( $\Delta\omega=0.25$  meV), the temperature below which the elastic magnetic scattering develops around  $(\pi, \pi)$ . Thus a revised magnetic phase diagram in the lightly doped region of  $\text{La}_{2-x}\text{Sr}_x\text{CuO}_4$  is proposed. The Curie constants calculated from the in-plane susceptibility are independent of the Sr concentration. On the basis of the cluster spin-glass model, this fact might reflect an inhomogeneous distribution of doped holes in the  $\text{CuO}_2$  plane, such as in a stripe structure.

### I. INTRODUCTION

The single-layered high-temperature superconducting (hereafter abbreviated as HTSC) 2-1-4-type cuprates have received intensive attention in explorations not only of the microscopic HTSC mechanism but also of the basic properties of two-dimensional magnetism in the square-lattice Heisenberg antiferromagnet.<sup>1</sup> The three-dimensional (3D) antiferromagnetic (AF) long-range order in undoped  $\text{La}_2\text{CuO}_4$  quickly vanishes<sup>2</sup> with hole doping either through the substitution of  $\text{La}^{3+}$  sites with  $\text{Sr}^{2+}$  or by the insertion of the excess oxygen. Upon further doping, the  $\text{La}_{2-x}\text{Sr}_x\text{CuO}_4$  (LSCO) system shows superconductivity in the range  $0.06\leq x\leq 0.25$  as well as incommensurate spin fluctuations.<sup>3,4</sup> Static spin correlations with the same incommensurability as those of dynamic one are also observed for the samples whose doping rates are near  $x=0.12$  (Refs. 5 and 6) and  $x=0.06$ .<sup>7</sup> In the intermediate regime,  $0.02\leq x\leq 0.05$ , placed between the 3D AF state and the superconducting state, there coexists a canonical spin-glass state observed by magnetic susceptibility measurements<sup>8</sup> and quasistatic magnetic order investigated by neutron-scattering experiments.<sup>9-11</sup> From the  $^{139}\text{La}$  nuclear quadrupole resonance (NQR) measurements, spin glass state with magnetically ordered finite-size regions, i.e., cluster spin glass state, is argued.<sup>12</sup> It is also reported that spin glass freezing temperature determined by the  $^{139}\text{La}$  NQR measurements in this region is proportional to  $1/x$ .<sup>13</sup> Very recently, Wakimoto *et al.*<sup>14</sup> found that the quasistatic magnetic order for  $x=0.05$  has an incommensurate structure whose modulation vector is along the orthorhombic  $b$  axis,  $\sim 45^\circ$  away from the incommensurate modulation observed in superconducting samples. Furthermore, an extensive study by Matsuda *et al.*<sup>15</sup> has revealed that the same type of incom-

mensurate spin structure exists throughout the hole concentration range  $0.024\leq x\leq 0.05$ .

From numerical simulations Gooding *et al.*<sup>16</sup> explained the coexistence of the spin-glass state and quasistatic magnetic order as a cluster spin-glass state taking into account hole localization around Sr ions. However, important unresolved problems exist for the physics in this intermediate doping region. One issue is how the incommensurate magnetic state is realized in the spin-glass state. For example, the model proposed by Gooding *et al.* predicts commensurate spin correlations in this region. Therefore a new model for the spin state seems needed. Another important question is how the spin-glass state changes from the insulating region ( $x\leq 0.05$ ) to superconducting region ( $x\geq 0.06$ ). In spite of the dramatic change of the quasistatic correlations at the insulator-superconductor boundary from a diagonal incommensurate state, which is modulated along the diagonal line of the  $\text{CuO}_2$  square lattice, to a collinear incommensurate one, which is modulated along the collinear line of the  $\text{CuO}_2$  square lattice, systematic muon spin-resonance ( $\mu\text{SR}$ ) studies<sup>17</sup> have revealed that the spin freezing temperature, corresponding to the spin-glass transition, changes continuously across the boundary. Thus it is important to clarify whether the spin-glass state is essential for the superconductivity in this system.

In the present study, focusing on these unresolved issues, we have performed systematic magnetic susceptibility measurements on single crystals with  $x=0.03, 0.04, \text{ and } 0.05$  and have determined the magnetic phase diagram of the lightly doped region from both the bulk susceptibility and recent neutron-scattering experiments.<sup>11</sup> The contents of this paper are as follows: the theoretical background of the spin-glass features, including a scaling hypothesis of the spin-glass or-

der parameter, is presented in Sec. II. Section III describes sample preparation and experimental details. The results of the magnetic susceptibility measurements and a revised magnetic phase diagram are presented in Sec. IV. In Sec. V we discuss interpretations for some of the remarkable features we find, combining the susceptibility with previous neutron-scattering and  $\mu$  SR measurements.

## II. FEATURES OF THE CANONICAL SPIN-GLASS ORDER PARAMETER

Determination of the spin-glass state is not an easy task, since the effects of randomness do not appear to be unique. Furthermore the effect of frustration by doped holes in the LSCO system should be very strong due to the strong superexchange interaction in the antiferromagnetic lattice in each  $\text{CuO}_2$  plane. If the formation of the spin-glass state is commonly visible in a certain hole concentration range, we can expect that a strong local singlet formation between spins of doped holes at oxygen sites and nearest-neighbor  $\text{Cu}^{2+}$  spins must be an essential ingredient of the HTSC mechanism in this material.

In this paper we first demonstrate that the magnetic system we treat is a quenched spin-glass system, with holes introduced by random substitution of La site with Sr cations. Note that another doping case by an insertion of excess oxygens is supposed to be an annealed system, where the doped oxygens are staged and also ordered in each staged layer at slow cooling stage.<sup>18,19</sup>

In the quenched spin-glass system, magnetic susceptibility is postulated to result from the sum of a temperature-independent residual susceptibility and a Curie-type magnetic susceptibility:

$$\chi = \chi_0 + \frac{C}{T}(1 - q), \quad (1)$$

where  $\chi_0$  is temperature-independent susceptibility,  $C$  is the Curie constant, and  $q$  is the spin-glass order parameter. Thus nonzero spin-glass order parameter  $q$  gives rise to deviations of the magnetic susceptibility from simple Curie law behavior below the spin-glass transition temperature  $T_g$ . Usually the thermal evolution of  $\chi$  shows a distinct cusp at  $T_g$  which is characterized as a typical spin-glass feature.

More rigorously, the spin-glass order parameter should obey the scaling relation<sup>20</sup> described as

$$q = |t|^\beta \cdot f_\pm(H^2|t|^{-\beta-\gamma}), \quad (2)$$

$$t = \frac{T - T_g}{T_g}, \quad (3)$$

where  $H$  is applied magnetic field,  $\beta$  and  $\gamma$  are critical exponents, and  $T_g$  is spin-glass transition temperature. The scaling functions  $f_+$  and  $f_-$  are defined for  $T > T_g$  and  $T < T_g$ , respectively. The critical exponents,  $\beta$  and  $\gamma$ , should be compared with the values deduced by the renormalization-group theory of  $0.5 < \beta < 1$  and  $\gamma = 3 \pm 1$ . In fact, earlier measurements of Chou *et al.*<sup>8</sup> showed that the spin-glass state of the  $\text{La}_{1.96}\text{Sr}_{0.04}\text{CuO}_4$  sample obeys the scaling relation with  $\beta \sim 0.9$  and  $\gamma \sim 4.3$ . These results stand as an important reference for the present experiments. (Based

on their results, we reevaluated the hole concentration of the sample used by Chou *et al.* and find a value somewhat lower than the quoted  $x = 0.04$ ; see Sec. IV.)

Another important piece of evidence for the spin-glass state is the remanent magnetization below  $T_g$  when an external field is turned off after crossing  $T_g$  (field-cooling effect). It shows the distinct difference of the magnetic susceptibilities between the zero-field-cooling and field-cooling process below  $T_g$ . After the external field is switched off, the remanent magnetization typically relaxes following a stretched exponent function of time  $\tau$ ,

$$M(\tau) = M(0)\exp[\alpha\tau^{(1-n)}]. \quad (4)$$

Theoretical predictions give  $1 - n = 1/3$ , which is often found in typical spin-glass compounds. In fact, we confirm that the stretching exponent for the magnetization memories of the present crystals have the same values as in the experiments reported in Ref. 8.

## III. SAMPLE PREPARATION AND EXPERIMENTAL DETAILS

Single crystals of  $\text{La}_{2-x}\text{Sr}_x\text{CuO}_4$  with  $x = 0.03, 0.04,$  and  $0.05$  were grown by TSFZ (traveling-solvent floating-zone) method using a standard floating-zone furnace with some improvements.<sup>21</sup> Dried powders of  $\text{La}_2\text{O}_3$ ,  $\text{SrCO}_3$ , and  $\text{CuO}$  of 99.99% purity were used as starting materials for feed rods and solvent. The starting materials were mixed and baked in air at 850, 950, and 1000 °C for 24 h each with a thorough grinding between each baking. After this process, we confirmed by x-ray powder diffraction that the obtained powder samples consisted only of a single 2-1-4 phase. Solvents with the composition of  $\text{La}_{2-x}\text{Sr}_x\text{CuO}_4:\text{CuO} = 35:65$  in molar ratio were utilized in all growths. The growth conditions were basically the same as those used for the  $x = 0.15$  crystal reported in Ref. 19 except that excess  $\text{CuO}$  of  $\sim 1$  mol% was added into the feed rods to increase their packing density as well as to compensate the loss of  $\text{CuO}$  vaporizing in the melting process. The final crystals were typically 6 mm in diameter and 30 mm in length.

In order to characterize the Sr concentration of each crystal, the  $c$ -axis lattice constant was measured by x-ray powder diffraction. We found that lightly doped LSCO crystals tend to become oxygenated by the oxygen atmosphere of the melt-grown process; therefore the as-grown crystals were annealed in flowing Ar at 900 °C for 12 h so as to reach the stoichiometric oxygen content before the x-ray-diffraction measurements. In fact, an iodometric titration analysis on the  $x = 0.03$  crystal revealed that the oxygen content of the Ar-annealed crystal is closer to the stoichiometric oxygen content than that of the as-grown crystal. Figure 1 shows the dependence of the  $c$ -axis lattice constant on hole concentration. The data for  $x \geq 0.06$  (open circles) are from Ref. 3, and the results for the present crystals are plotted by closed circles. In addition, data for  $x = 0$  was determined from a single crystal of  $\text{La}_2\text{CuO}_4$  that was grown by the method reported in Ref. 19 and annealed in Ar atmosphere at 900 °C for 12 h. As clearly shown in Fig. 1, the  $c$ -axis lattice constants of the lower doped samples extrapolate smoothly from the published data. This smooth extrapolation indicates that

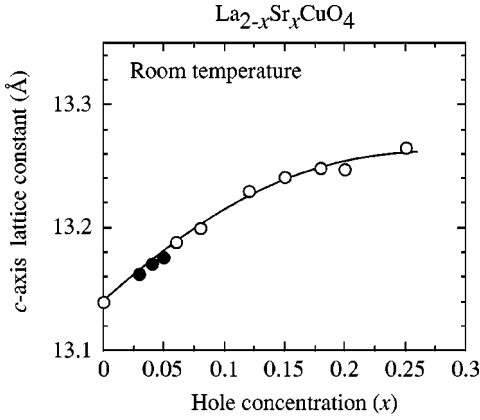


FIG. 1. Variation of the  $c$ -axis lattice constant versus hole concentration at the room temperature. Closed circles are data of the present crystals. Open circles, except for  $x=0$ , are data from Yamada (Ref. 3). The value at  $x=0$  was measured using a single crystal annealed in Ar atmosphere. The solid line is a guide to the eye.

the hole concentration of our crystals correspond closely to the expected values of  $x=0.03$ ,  $0.04$ , and  $0.05$ . We note that our results are subtly lower than the powder sample data reported by Takayama-Muromachi *et al.*<sup>22</sup> in the region of  $x \leq 0.06$ . We speculate that this small difference is caused by an effect of the Ar annealing performed on the present crystals.

The magnetic susceptibility measurements were performed using a standard Quantum Design superconducting quantum interference device (SQUID) magnetometer. Measurements were made on each crystal under various applied fields in the range  $0.02 \leq H \leq 5$  T either parallel or perpendicular to the  $\text{CuO}_2$  planes. We did not specify the field direction within the plane. Data were measured either by cooling with the field applied (FC) or by applying field after cooling in zero field (ZFC). Note that the  $\text{CuO}_2$  plane corresponds to the  $a$ - $b$  plane of the orthorhombic  $Bmab$  crystallographic notation, which is utilized throughout the paper.

#### IV. MAGNETIC SUSCEPTIBILITY

For all of the samples we studied, the magnetic susceptibility under a magnetic field parallel to the  $\text{CuO}_2$  plane, which we call in-plane magnetic susceptibility, exhibits qualitatively the same temperature dependence. As a typical example Fig. 2(a) shows the temperature dependence of the in-plane susceptibility of the  $x=0.03$  sample. A clear difference exists between the FC and ZFC data corresponding to hysteresis characteristic of spin glasses. The inset of Fig. 2(a) shows the time dependence of the remanent magnetization after turning off an applied field of 1 T. This time dependence is well fit by Eq. (4) with  $1-n=1/3$  (solid line). These facts provide a direct evidence that a canonical spin-glass state exists in the  $\text{CuO}_2$  planes in this system.

Below the spin-glass transition temperature  $T_g$  the magnetic susceptibility starts to deviate from Curie law, as indicated by a dashed line in Fig. 2(a). The dashed line of the Curie law was calculated by a least-squares fit to the data between 10 and 70 K. The spin-glass order parameter  $q$  can be evaluated from the degree of the deviation using Eq. (1).

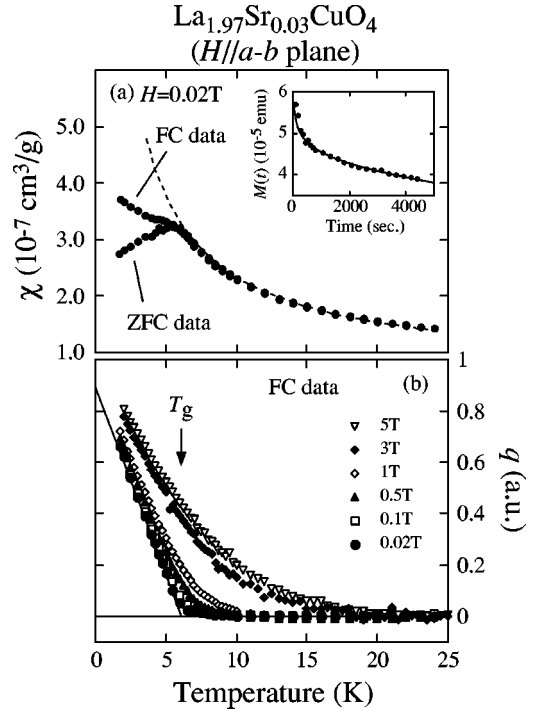


FIG. 2. (a) Temperature dependence of the in-plane magnetic susceptibility for the  $x=0.03$  sample. A magnetic field of 0.02 T was applied parallel to the  $\text{CuO}_2$  planes. Both ZFC and FC data are included. A dashed line indicates the Curie law corresponding to the susceptibility with  $q=0$  as determined by a least-square fitting at higher temperatures ( $10 \leq T \leq 70$  K). The inset shows a time dependence of the remanent magnetization. The solid line is a least-square fit to Eq. (4). (b) Temperature dependence of spin-glass order parameter  $q$  determined from the FC data by Eq. (1) at several applied fields ( $0.02 \leq H \leq 5$  T). The solid line is a least-square fit of the  $H=0.02$  T data to the equation of  $q \propto (T_g - T)^\beta$ .

Figure 2(b) shows the thermal variation of  $q$  calculated from the FC data in various applied fields.  $T_g$  was determined by a least-square fit to the temperature dependence of  $q$  at  $H=0.02$  T using the equation  $q \sim (T_g - T)^\beta$ . The solid line in Fig. 2(b) shows the result of the fit with  $T_g = 6.3(\pm 0.5)$  K and  $\beta = 0.97(\pm 0.05)$ . Similarly,  $T_g$  for the  $x=0.04$  and  $0.05$  samples are determined to be  $5.5(\pm 0.5)$  and  $5.0(\pm 0.5)$  K with the same value of  $\beta$ , respectively.

To characterize further the spin-glass properties in this system, we verify the scaling hypothesis described by Eq. (2). Figure 3 shows the scaling of the in-plane magnetic susceptibility. The scaling relation is well satisfied for all samples with the same value of the critical exponents. This fact indicates that the spin-glass behavior in the in-plane susceptibility is common to the  $x=0.03$ ,  $0.04$ , and  $0.05$  samples, and that these samples exhibit a canonical quenched spin-glass state. Furthermore, the critical exponents  $\beta$  and  $\gamma$  obtained from the universal plots are  $0.97(\pm 0.05)$  and  $3.2(\pm 0.5)$ , which are consistent with those of typical canonical spin-glass materials.

In contrast, the magnetic susceptibility under a magnetic field along the out-of-plane direction, which we call out-of-plane magnetic susceptibility, shows behavior different from typical spin glasses. The temperature dependence of the out-of-plane susceptibility of the  $x=0.03$  sample is shown in Fig. 4(a) as an example. A difference between FC and ZFC

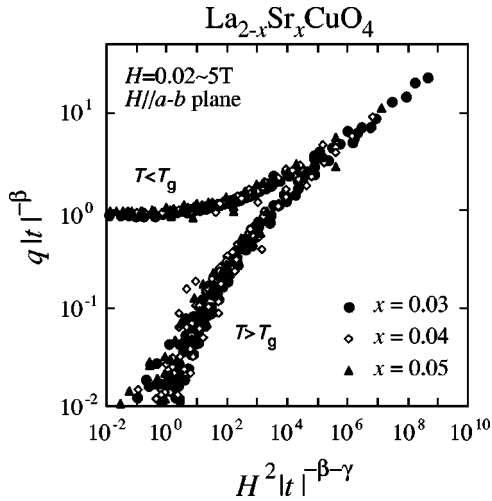


FIG. 3. Universal curves plotted for the scaling relation of Eq. (2) using the in-plane FC data from the  $x=0.03$ ,  $0.04$ , and  $0.05$  samples with applied fields of  $0.02 \leq H \leq 5$  T. The spin-glass exponents  $\beta$  and  $\gamma$  are  $0.97(\pm 0.05)$  and  $3.2(\pm 0.5)$ , respectively.

data is observable at low  $T$ , and a small shoulder appears at  $T_g$  determined by the in-plane measurements. These features of the out-of-plane susceptibility are qualitatively similar to those of the in-plane spin-glass behavior. However, a remarkable difference is that the out-of-plane susceptibility deviates from a simple Curie law at a temperature well above  $T_g$ , as clearly shown in Fig. 4(a). Such a deviation is ob-

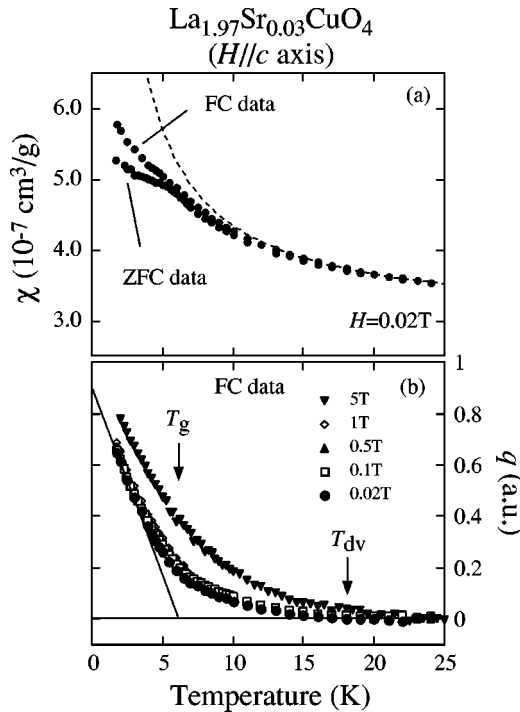


FIG. 4. (a) Temperature dependence of the out-of-plane magnetic susceptibility of the  $x=0.03$  sample. A magnetic field of  $0.02$  T was applied perpendicular to the  $\text{CuO}_2$  planes. The dashed line shows the Curie law corresponding to a susceptibility with  $q=0$ . (b) Temperature dependence of spin-glass order parameter  $q$  calculated from the FC data at several applied fields ( $0.02 \leq H \leq 5$  T). The solid line is a fit result of the in-plane data. The arrow indicates  $T_g$  determined by the in-plane data.

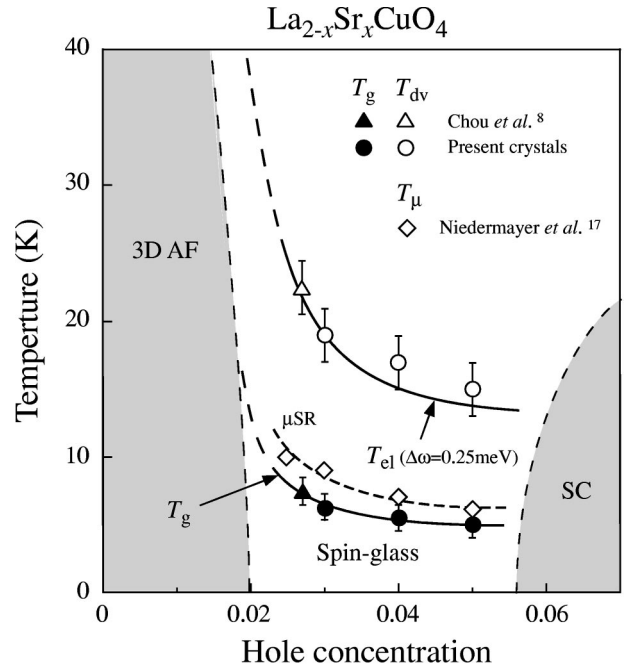


FIG. 5. Magnetic phase diagram for the lightly doped region. The circles are the data of the present crystals and the triangles are those reported by Chou *et al.* (Ref. 8). Closed and open symbols indicate  $T_g$  and  $T_{dv}$ , respectively, as determined by the magnetic susceptibility measurements. The line for  $T_g$  is a guide to the eye and the line for  $T_{el}$  is from Ref. 11. Open diamonds indicate the temperatures where magnetic signals are observed in the  $\mu\text{SR}$  measurements (Ref. 17).

served in all the samples and was also reported by Chou *et al.*<sup>8</sup> This deviation indicates that, under the same analysis as for the in-plane susceptibility,  $q$  increases from zero far above  $T_g$ . This feature is more clearly visible in a calculation of  $q$  from the FC data, as shown in Fig. 4(b). The onset temperatures for these deviations,  $T_{dv}$ , are found to be  $19(\pm 2)$ ,  $17(\pm 2)$ , and  $15(\pm 2)$  K for  $x=0.03$ ,  $0.04$ , and  $0.05$ , respectively. In addition, the spin-glass order parameter of the out-of-plane magnetic susceptibility does not obey the scaling relation of Eq. (2). This result suggests that another magnetic mechanism rather than spin-glass behavior drives the deviation of the out-of-plane susceptibility from the simple Curie-type paramagnetic behavior.

We summarize the magnetic susceptibility data in Fig. 5 with a magnetic phase diagram that includes results from Chou *et al.*<sup>8</sup> on an  $x=0.04$  crystal and  $\mu\text{SR}$  results reported by Niedermayer *et al.*<sup>17</sup> The closed and open circles indicate  $T_g$  and  $T_{dv}$  of the present crystals, respectively, while the closed and open triangles are those of the “ $x=0.04$ ” crystal of Chou *et al.* Previous reports on a sample of  $\text{La}_{2-x}\text{Bi}_x\text{CuO}_{4+\delta}$  whose hole concentration is just above the boundary of 3D AF state showed a spin-glass transition with  $T_g \approx 17$  K,<sup>23</sup> therefore we draw an  $x$  dependence line of  $T_g$  as a guide to the eye which reaches 17 K at  $x=0.02$ . From this line, the actual hole concentration of the “ $x=0.04$ ” sample of Chou *et al.* can be estimated to be  $0.027$ .<sup>24</sup> Thus we treat the data of Chou *et al.* as  $x=0.027$  in the present paper.

According to the recent neutron-scattering experiments reported by Wakimoto and co-workers<sup>11,14</sup> using the same crystals as those in the present experiment, elastic incom-

mensurate magnetic peaks exist around the  $(\pi, \pi)$  position in reciprocal space. The solid line of  $T_{el}(\Delta\omega=0.25 \text{ meV})$  in Fig. 5 shows the  $x$  dependence of the onset temperature where the elastic magnetic peaks become observable with the energy resolution of  $\Delta\omega=0.25 \text{ meV}$ .  $T_{dv}$  exhibits qualitatively the same  $x$  dependence as that of  $T_{el}(\Delta\omega=0.25 \text{ meV})$ . The physical meaning of this feature is discussed in the next section.

The temperatures below which a magnetic signal is observed in the  $\mu$  SR measurements of Niedermayer *et al.*<sup>17</sup> are also plotted as open diamonds in Fig. 5. (Hereafter, we label these temperatures as  $T_\mu$ .) Niedermayer *et al.* equated  $T_\mu$  with the spin-glass transition temperature. However, in our phase diagram, there is a small discrepancy between  $T_\mu$  and  $T_g$ . Our  $T_g$  values for  $x=0.03$  and  $0.04$  are very close to the spin-glass freezing temperature determined by the <sup>139</sup>La NQR measurements in Ref. 13. We believe that the differences among  $T_{el}$ ,  $T_\mu$ , and  $T_g$  arise from the differences in the observation time scales for the different experimental methods. In fact, Keimer *et al.*<sup>10</sup> reported that  $T_{el}$  depends on the instrumental energy resolution, which varies inversely with observation time scale. Furthermore, the nature of the magnetic susceptibility measured by SQUID is perfectly static. These facts indicate that the magnetic correlations in this system are essentially quasistatic, and, specifically, that with decreasing temperature the spin system freezes into a cluster spin-glass state consisting of domains in which spins are antiferromagnetically correlated.

## V. DISCUSSION

The present results of the magnetic susceptibility measurements have revealed the existence of a common canonical spin-glass state for  $\text{La}_{2-x}\text{Sr}_x\text{CuO}_4$  in the insulating region of  $0.03 \leq x \leq 0.05$ . In this section, we discuss the nature of the spin correlations specifically to reconcile this finding with the recent neutron-scattering results on samples in the same hole concentration range.

First, we discuss the  $x$  dependence of the characteristic temperatures  $T_g$ ,  $T_{el}$ , and  $T_{dv}$ . In Fig. 5, all of these temperatures exhibit qualitatively similar  $x$  dependences. Since the difference between  $T_g$  and  $T_{el}$  reflects the different time scales of the experimental probes in observing the freezing spin system, the similarity between the  $x$  dependences of  $T_g$  and  $T_{el}$  indicates that the freezing process into the cluster glass state is similar for the samples in this hole concentration range. Although the  $T_{dv}$  values sit on the  $T_{el}(\Delta\omega=0.25 \text{ meV})$  line, the significant feature is not their equivalent values but their qualitatively similar  $x$  dependence. As mentioned in Sec. IV, the position of  $T_{el}$  is arbitrary to the extent that it depends on the instrumental energy resolution width  $\Delta\omega$ . The similar  $x$  dependences of  $T_{dv}$  and  $T_{el}$  suggest a correlation between the formation of the spin clusters and the deviation of the out-of-plane susceptibility from simple Curie-type behavior. There may also be a relation between this deviation from the Curie law and the development of short magnetic correlations along the out-of-plane direction as observed by neutron-scattering measurements for  $x=0.03$  and  $0.05$  at low temperature.<sup>11,14</sup>

Next, we discuss the spin-glass properties of the in-plane magnetic susceptibility, particularly, the  $x$  dependence of the

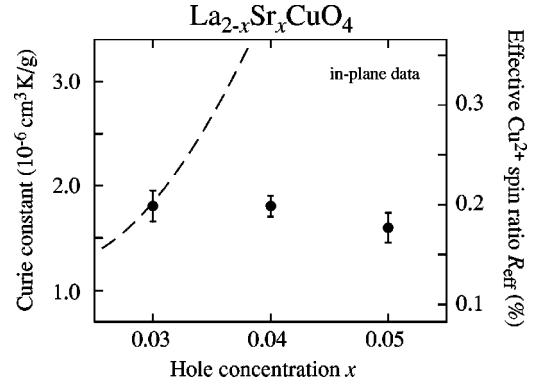


FIG. 6. Hole concentration dependence of the Curie constant  $C$  determined by the least-square fit to the in-plane magnetic susceptibility data. The left vertical axis shows the Curie constant while the right vertical axis shows the effective  $\text{Cu}^{2+}$  spin ratio  $R_{eff}$ . A dashed line corresponds to the theoretical prediction by Gooding *et al.* (Ref. 16) (see text).

Curie constant shown in Fig. 6. The Curie constants, calculated from a least-square fit to the in-plane susceptibility data between 10 and 70 K, are essentially independent of  $x$  for this hole concentration range. The right vertical axis of Fig. 6 indicates the scale of the ratio  $R_{eff} = N_{eff}/N_{all}$ , where  $N_{eff}$  is the number of effective  $\text{Cu}^{2+}$  spins giving the simple Curie-type paramagnetic susceptibility and  $N_{all}$  is the total number of  $\text{Cu}^{2+}$  spins per unit volume.  $N_{eff}$  is related to the Curie constant by the following formula:

$$C = N_{eff} \frac{(g\mu_B)^2 S(S+1)}{3k_B}, \quad (5)$$

where  $g=2$ ,  $S=1/2$ , and  $k_B$  is Boltzmann's constant.

As pointed out by Gooding *et al.*,<sup>16</sup> if the cluster spin-glass state is realized in this system, each cluster consisting of an odd number of spins behaves like a single spin yielding a Curie-type paramagnetic behavior. Hence the number of effective  $\text{Cu}^{2+}$  spins should be half of the total number of the clusters. Therefore  $R_{eff}$  can be described using an average cluster size  $L$  (expressed in the unit of the nearest-neighbor Cu-Cu distance) as

$$R_{eff} = \frac{1}{2L^2}. \quad (6)$$

From a numerical calculation, Gooding *et al.*<sup>16</sup> reported that  $L$  is given by  $L = Ax^{-\eta}$  ( $A \sim 0.49$  and  $\eta \sim 0.98$ ) on the basis of the cluster spin-glass model with a random distribution of doped holes. In this model, the doped holes form the boundaries between the clusters. Their result is indicated by a dashed line in Fig. 6. Although the  $R_{eff}$  value for  $x=0.03$  is close to the prediction of Gooding *et al.*, the  $R_{eff}$  values are independent of  $x$ , with those for  $x=0.04$  and  $0.05$  significantly smaller than the dashed line. The constant value of  $R_{eff}$  combined with Eq. (6), means that the cluster size is independent of the hole concentration, instead of decreasing with increasing doping level as predicted for a random distribution of holes located on the cluster boundary.

A possible interpretation of these features is that the doped holes are distributed also inside the clusters as well as on the boundaries. Recent neutron-scattering results<sup>14,15</sup>

demonstrate that quasistatic incommensurate spin correlations exist in the spin-glass region. This may imply that the holes inside the clusters form charge stripes and each cluster includes antiphase antiferromagnetic domains divided by these charge stripes. In this model, the  $x$ -independence of the cluster size suggests that only the distance between nearest-neighbor charge stripes (i.e.,  $1/\text{incommensurability}$ ) within the clusters varies with the hole concentration. Consistent with this picture, the incommensurability of the quasielastic peaks observed by neutron-scattering experiments<sup>14,15</sup> increases linearly with the hole concentration  $x$  in the spin-glass region where we observe no change in the Curie constant. The mechanism of cluster boundary formation is still an open question. Possible constituents of the cluster boundary are, for example, a small amount of holes distributed outside the charge stripes or displacements of the stripes. A correct model for the cluster glass state including charge stripes needs further clarification.

Briefly, we should note another possibility for the discrepancy between the theoretical line and the present results for  $R_{eff}$ . In the model of Gooding *et al.*, the spin-glass cluster size is supposed to be equivalent to the instantaneous magnetic correlation length. However, the  $R_{eff}$  values correspond to a time-averaged cluster size rather than instantaneous one since the  $R_{eff}$  values are obtained by magnetic susceptibility measurements. Additional careful investigations are required to distinguish the static from dynamic magnetic properties.

To conclude, the present results combined with recent neutron-scattering and  $\mu$ SR measurements indicate that the spin system for  $\text{La}_{2-x}\text{Sr}_x\text{CuO}_4$  in the range  $0.03 \leq x \leq 0.05$  freezes into a cluster spin-glass state at low temperatures while maintaining antiferromagnetically correlated spins in

each cluster. Inside the clusters, it is likely that the doped holes are inhomogeneously distributed. A stripe structure is suggested by the elastic incommensurate peaks observed in the neutron scattering.<sup>14,15</sup>

One of the remaining important issues is the role of the cluster spin-glass state with respect to the superconductivity in the  $\text{La}_{2-x}\text{Sr}_x\text{CuO}_4$  system. Since the  $x$  dependences of all the characteristic temperatures  $T_g$ ,  $T_{el}$ , and  $T_{dv}$  near the superconducting boundary are very small in Fig. 5, the spin-glass region may extend into the superconducting region as suggested by Niedermayer *et al.*<sup>17</sup>. In fact, neutron scattering reveals quasistatic incommensurate peaks in underdoped superconducting samples which may relate the spin-glass phase within the superconducting state.<sup>7</sup> However, the spatial spin modulation of the spin-glass state in the superconducting phase should differ from that of the spin-glass phase in the nonsuperconducting state as demonstrated by recent neutron scattering.<sup>7</sup> In order to clarify the role of the cluster spin-glass state in the HTSC mechanism, further investigations are necessary of the spin-glass features in the superconducting region compared with those in the insulating region.

#### ACKNOWLEDGMENTS

We gratefully thank R. J. Birgeneau, F. C. Chou, K. Hirota, Y.-J. Kim, Y. S. Lee, R. Leheny, S. Maekawa, G. Shirane, and S. M. Shapiro for invaluable discussions. We also thank M. Onodera for his technical assistance. The present work has been supported by a Grant-in-Aid for Scientific Research from the Japanese Ministry of Education, Science, Sports and Culture, by a Grant for the Promotion of Science from the Science and Technology Agency, and by the Core Research for Evolutional Science and Technology (CREST).

\*Present address: Massachusetts Institute of Technology, Cambridge, MA 02139.

<sup>1</sup>M. A. Kastner, R. J. Birgeneau, G. Shirane, and Y. Endoh, *Rev. Mod. Phys.* **70**, 897 (1998).

<sup>2</sup>A. Aharony, R. J. Birgeneau, A. Coniglio, M. A. Kastner, and H. E. Stanley, *Phys. Rev. Lett.* **60**, 1330 (1988).

<sup>3</sup>K. Yamada, C. H. Lee, K. Kurahashi, J. Wada, S. Wakimoto, S. Ueki, H. Kimura, Y. Endoh, S. Hosoya, G. Shirane, R. J. Birgeneau, M. Greven, M. A. Kastner, and Y. J. Kim, *Phys. Rev. B* **57**, 6165 (1998).

<sup>4</sup>For samples with  $x \approx 0.15$ , the incommensurate spin fluctuation is reported in, for example, H. Yoshizawa, S. Mitsuda, H. Kitazawa, and K. Katsumata, *J. Phys. Soc. Jpn.* **57**, 3686 (1988); R. J. Birgeneau, Y. Endoh, Y. Hidaka, K. Kakurai, M. A. Kastner, T. Murakami, G. Shirane, T. R. Thurston, and K. Yamada, *Phys. Rev. B* **39**, 2868 (1989); S.-W. Cheong, G. Aeppli, T. E. Mason, H. A. Mook, S. M. Hayden, P. C. Canfield, Z. Fisk, K. N. Klausen, and J. L. Martinez, *Phys. Rev. Lett.* **67**, 1791 (1991); T. E. Mason, G. Aeppli, S. M. Hayden, A. P. Ramirez, and H. Mook, *ibid.* **71**, 919 (1993); M. Matsuda, K. Yamada, Y. Endoh, T. R. Thurston, G. Shirane, R. J. Birgeneau, M. A. Kastner, I. Tanaka, and H. Kojima, *Phys. Rev. B* **49**, 6958 (1994).

<sup>5</sup>T. Suzuki, T. Goto, K. Chiba, T. Shinoda, T. Fukase, H. Kimura, K. Yamada, M. Ohashi, and Y. Yamaguchi, *Phys. Rev. B* **57**, 3229 (1998).

<sup>6</sup>H. Kimura, K. Hirota, H. Matsushita, K. Yamada, Y. Endoh, S.

H. Lee, C. F. Majkrzak, R. Erwin, G. Shirane, M. Greven, Y. S. Lee, M. A. Kastner, and R. J. Birgeneau, *Phys. Rev. B* **59**, 6517 (1999).

<sup>7</sup>S. Wakimoto, K. Yamada, S. Ueki, G. Shirane, Y. S. Lee, S. H. Lee, M. A. Kastner, K. Hirota, P. M. Gehring, Y. Endoh, and R. J. Birgeneau, *J. P. Chem. Solids* **60**, 1079 (1999).

<sup>8</sup>F. C. Chou, N. R. Belk, M. A. Kastner, and R. J. Birgeneau, *Phys. Rev. Lett.* **75**, 2204 (1995).

<sup>9</sup>S. M. Hayden, G. Aeppli, H. Mook, D. Rytz, M. F. Hundley, and Z. Fisk, *Phys. Rev. Lett.* **66**, 821 (1991).

<sup>10</sup>B. Keimer, N. Belk, R. J. Birgeneau, A. Cassanho, C. Y. Chen, M. Greven, M. A. Kastner, A. Aharony, Y. Endoh, R. W. Erwin, and G. Shirane, *Phys. Rev. B* **46**, 14 034 (1992).

<sup>11</sup>S. Wakimoto, G. Shirane, Y. Endoh, K. Hirota, S. Ueki, K. Yamada, R. J. Birgeneau, M. A. Kastner, Y. S. Lee, P. M. Gehring, and S. H. Lee, *Phys. Rev. B* **60**, R769 (1999).

<sup>12</sup>J. H. Cho, F. Borsa, D. C. Johnston, and D. R. Torgeson, *Phys. Rev. B* **46**, 3179 (1992).

<sup>13</sup>F. C. Chou, F. Borsa, J. H. Cho, D. C. Johnston, A. Lascialfari, D. R. Torgeson, and J. Ziolo, *Phys. Rev. Lett.* **71**, 2323 (1993).

<sup>14</sup>S. Wakimoto, R. J. Birgeneau, M. A. Kastner, Y. S. Lee, R. Erwin, P. M. Gehring, S. H. Lee, M. Fujita, K. Yamada, Y. Endoh, K. Hirota, and G. Shirane, *Phys. Rev. B* **61**, 3699 (2000).

<sup>15</sup>M. Matsuda, M. Fujita, K. Yamada, R. J. Birgeneau, M. A. Kastner, Y. Endoh, S. Wakimoto, and G. Shirane, cond-mat/0003466 (unpublished).

- <sup>16</sup>R. J. Gooding, N. M. Salem, R. J. Birgeneau, and F. C. Chou, Phys. Rev. B **55**, 6360 (1997).
- <sup>17</sup>Ch. Niedermayer, C. Bernhard, T. Blasius, A. Golnik, A. Moodenbaugh, and J. I. Budnick, Phys. Rev. Lett. **80**, 3843 (1998).
- <sup>18</sup>B. O. Wells, R. J. Birgeneau, F. C. Chou, Y. Endoh, D. C. Johnston, M. A. Kastner, Y. S. Lee, G. Shirane, J. M. Tranquada, and K. Yamada, Z. Phys. B: Condens. Matter **100**, 533 (1996).
- <sup>19</sup>X. Xiong, P. Wochner, S. C. Moss, Y. Cao, K. Koga, and M. Fujita, Phys. Rev. Lett. **76**, 2997 (1996).
- <sup>20</sup>Chou *et al.* (Ref. 8) evaluated this relation from the scaling hypothesis in a conventional spin glass material reported in the following papers: A. P. Malozemoff, S. E. Barnes, B. Barbara, Phys. Rev. Lett. **51**, 1704 (1983); B. Barbara, A. P. Malozemoff, and Y. Imry, *ibid.* **47**, 1852 (1981).
- <sup>21</sup>C. H. Lee, N. Kaneko, S. Hosoya, K. Kurahashi, S. Wakimoto, K. Yamada, and Y. Endoh, Supercond. Sci. Technol. **11**, 891 (1998).
- <sup>22</sup>E. Takayama-Muromachi and D. E. Rice, Physica C **177**, 195 (1991).
- <sup>23</sup>S. Wakimoto, K. Kurahashi, C. H. Lee, K. Yamada, Y. Endoh, and S. Hosoya, Physica B **237-238**, 91 (1997).
- <sup>24</sup>This re-estimation was also confirmed by a  $x$  dependence of  $T_{el}$  determined by the neutron-scattering experiments in Ref. 11.